Geomechanics and Engineering, *Vol. 39, No. 6 (2024) 629-645*
https://doi.org/10.12989/gae.2024.39.6.629

Impact of different temperature conditions on durability and microstructure of clay stabilized

Navid Khayat*[1], Ahad Nazarpour[2], Hadis Nasiri[1] and Anil Kumar Sharma[3]

[1]*Department of Civil Engineering, Ahvaz Branch, Islamic Azad University, Ahvaz, Iran*
[2]*Department of Geology, Ahvaz Branch, Islamic Azad University, Ahvaz, Iran*
[3]*Department of Civil Engineering, National Institute of Technology Patna, Patna, Bihar, India*

(*Received September 6, 2023, Revised December 10, 2024, Accepted December 16, 2024*)

Abstract. This study focuses on enhancing structural strength in flood-prone regions by utilizing industrial waste under varying temperature conditions. Industrial waste's increasing usage and its environmental implications require deeper comprehension. The escalating adoption of industrial waste as an alternative construction material underscores this shift. The research employs fly ash (F), ground-granulated blast-furnace slag (G), and lime (L) to augment geotechnical properties and bolster the flood resistance of stabilized soil. Various clay, lime, GGBS, and 2% fly ash mixtures are tested under optimal moisture and maximum dry density conditions. The curing spans 1, 7, 14, 28, 56, and 90 days at ambient temperature and 3°C. Subsequent unconfined compressive strength (UCS), durability, X-ray diffraction (XRD), energy-dispersive X-ray spectroscopy (EDS), and field emission scanning electron microscopy (FE-SEM) analyses are conducted. Results highlight a 257% UCS increase at 14 days' curing for the 8% GGBS + 6% Lime + 2% Fly ash mixture at ambient temperature, while the mix of 6% GGBS + 8% Lime + 2% Fly ash records a 686% UCS enhancement after 90 days' curing at 3°C. Lime concentration affects the plasticity index and maximum dry unit weight (MDU). Upon water immersion, durability testing indicates an 11-17% strength reduction for lime, GGBS, and fly ash samples. The microstructural evaluation identifies hydration products like calcium aluminate silicate-hydrate and calcium silicate hydrate. According to the findings, using industrial waste can be a promising solution to pavement sustainability, especially after the flood, and it can reduce related costs and decrease CO_2 emissions.

Keywords: durability; fly ash; lime; microstructural analysis; road engineering; temperature condition

1. Introduction

One of the concerns is whether the engineering infrastructure would still have the same strength after the floods subsided. Given that high-quality materials are not available on the construction site and should be transported from long distances, it is necessary to find solutions to improve the ground and reduce costs in road construction while considering environmental aspects (Khayat *et al.* 2023). Byproducts of steel industries are available and affordable in many parts of the world, including Khuzestan Province, Iran. These byproducts can provide a proper perspective of development in the province since they are efficient stabilizers in road construction (Sukprasert *et al.* 2021).

Disposal of large quantities of excess soil with weak geotechnical properties is a problem that construction companies deal with and has economic and environmental costs to transport them from the construction site. Using traditional additives such as lime and cement to improve the geotechnical properties of excess soil is considered an effective method that allows the application of additives at a given project site which is an appropriate solution (Al Haffar *et al.* 2021, Syed and GuhaRay 2020, Bruno *et al.* 2018).

Various methods for improving ground properties depend on improved efficiency and project conditions. A process can have advantages over others in terms of economic aspects, implementation conditions, facilities, and temporal and spatial limitations (Behnood 2018). Stabilizing soil is primarily aimed at modifying soils, accelerating construction, and improving soil strength and durability. Soil improvement may be aimed at increasing compressive strength or environmental load resistance. The induction of different reactions and alternating soil particle connectivity stabilize and strengthen the soil. In these reactions, particles transform into a new material with various properties (Gowthaman *et al.* 2021).

Lime is a common additive in soil stabilization (Haghighatjo and Zolfegharifar 2022). It is a product of limestone fires and changes into slaked lime by combining with water, retransforming into limestone by absorbing CO2 from the air. Lime exists in nature in the forms of quicklime (CaO) and slaked lime (Ca (OH) $_2$) (Alavéz-Ramírez *et al.* 2012). Although it is extensively used, quicklime has significant health and environmental impacts.

The reaction between lime and water is exothermic and produces gaseous CO_2, imposing health impacts (Nasiri *et al.* 2021). The modification of soil using lime increases the optimum moisture content (OMC), reduces the maximum dry unit weight (MDU) and swelling potential, and

*Corresponding author, Ph.D.
E-mail: navid.khayat@iau.ac.ir

ISSN: 2005-307X (Print), 2092-6219 (Online)

Fig. 1 A view of Ahvaz-Shush road after the flood in 2019

enhances strength and elasticity modulus (Moayyeri *et al*. 2019).

On the other hand, when the soil contains sulfate ions or the stabilized soil is subjected to sulfated water, lime shows the opposite impact. It increases the swelling of the stabilized soil layer due to ettringite formation (Aldaood *et al.* 2014). This stems from chemical reactions between clay minerals, lime, and sulfate, forming ettringite. Expansion caused by the growth of ettringite in sulfate soils may produce severe problems in the construction and performance of pavement foundation systems (Ferris *et al.* 1991).

Due to environmental concerns, there has recently been an increasing tendency to utilize industrial waste as an alternative to construction materials (Mohanty *et al.* 2017). It has many applications for the disposal of industrial waste.

The mechanical stabilization of swelling clay soil using ground-granulated blast-furnace slag (GGBS) is an affordable, efficient, and environmentally friendly method that helps mitigate industrial waste disposal impacts (Pai *et al*. 2020). Furthermore, soil stabilization using industrial products such as fly ash, GGBS, mine waste, and stone waste powder in mixtures with lime and cement has been shown to have good outcomes in improving the geotechnical properties of problematic soils (Ramesh *et al.* 2022, Thomas *et al.* 2019, Cristelo *et al.* 2013, Chen and Lin 2009, Bilgin *et al.* 2012). GGBS modifies the geotechnical parameters, enhances soil's unconfined compressive strength (UCS), and provides cost-efficiency. It is a non-metal product of steel industries and consists of SiO_2, Ca_2O_4Si, and Al_2O_3 (Zhuang and Wang 2021). GGBS possesses cementitious properties that can substitute for a portion of lime in soil stabilization. Adding GGBS to lime-stabilized clay in the presence of sulfate can reduce the undesired impacts of sulfate and improve strength (Lang *et al.* 2021). Fly ash is a byproduct of thermal power plants. It is captured in thermal power plants using electrostatic precipitators. Approximately 100,000 tons of fly ash are produced annually around the world. Fly ash significantly improves the chemical properties of lime-stabilized soil (Rikmann *et al.* 2021). Chenari *et al.* (2018) demonstrated that adding fly ash to soil significantly enhanced the strength of the soil samples.

In our study, we aimed to investigate the stabilization of soils under varying temperature conditions using fly ash, GGBS, and lime. This approach stands out because it focuses on temperature's role in stabilization processes, a less-explored factor in soil improvement studies. While previous studies like Mishra *et al*. (2022) and Nasiri *et al.* (2021) focused on using agricultural and industrial by-products for expansive soil stabilization, they primarily evaluated the geotechnical behavior under constant ambient conditions. On the other hand, our research included a detailed examination of stabilization at two different temperature levels, addressing both ambient and low-temperature conditions (3°C), which is crucial for flood-prone regions with cold climates. Furthermore, Sharma and Hymavathi (2016) demonstrated the beneficial effects of fly ash and lime combinations on clayey soils. However, their research did not address the long-term durability of these stabilizers under extreme environmental conditions, such as water immersion or cold climates, which is a key aspect covered in our study. By introducing different lime and GGBS percentages and subjecting them to varied curing periods, we observed that GGBS and fly ash mixtures exhibited stronger pozzolanic reactions, providing superior durability, particularly under cold conditions. This observation aligns with the findings by Parhizkar *et al.* (2024), who similarly noted the limited effectiveness of increasing fly ash content beyond 2% for soil stabilization. Finally, Mishra *et al.* (2022) emphasized the use of by-products like fly ash and GGBS, but the novelty in our work lies in combining these additives and assessing their performance across a range of conditions. Our study's 3°C curing conditions represent an original contribution, further validated by our comprehensive microstructural analysis using XRD and SEM techniques. These findings, alongside our comparisons with other studies, clarify the distinct benefits of using specific additive combinations in cold environments, offering a fresh perspective on sustainable soil stabilization strategies.

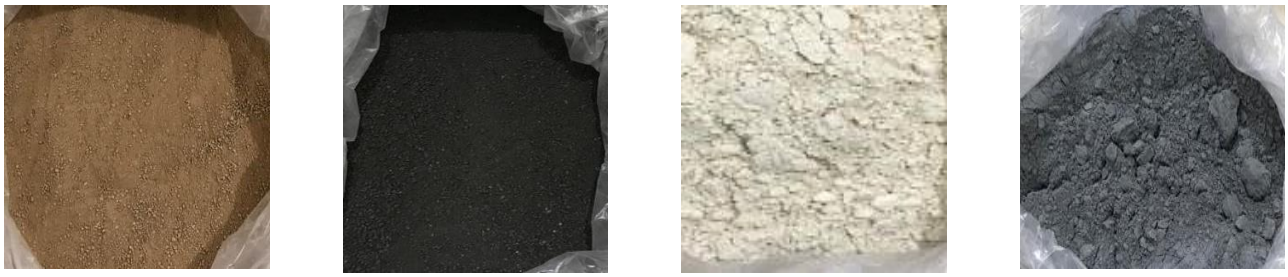

(a) (b) (c) (d)

Fig. 2 A view of (a) Soil, (b) GGBS, (c) Lime and (d) Fly ash

Table 2 Chemical compositions of soil, lime, fly ash and GGBS used in this study

Oxide concentration (%)	Chemical compositions by weight (%)			
	Soil	Lime	Fly ash	GGBS
SiO_2 (Silica)	23.43	2.67	96.4	17.16
Al_2O_3 (Alumina)	6.12	0.752	1.32	3.57
CaO (Calcium oxide)	32.12	63.67	0.49	31.81
Fe_2O_3 (Iron oxide)	2.68	0.51	0.87	32.39
K_2O (Potassium oxide)	1.25	0.27	1.01	0.06
MgO (Magnesium oxide)	3.55	3.74	0.97	13.07
MnO (Manganese oxide)	0.05	-	-	0.27
Na_2O (Sodium oxide)	0.67	0.05	0.31	0.37
P_2O_5 (Phosphorus pentoxide)	0.17	0.03	0.1	0.11
SO_3 (Sulphur oxide)	0.29	0.91	0.16	0.10
TiO_2 (Tin oxide)	0.32	0.05	-	1.09
Loss on Ignition	29.22	-	-	-

Table 1 Geotechnical properties of clay soil

Grain-size distribution (ASTM D422)	
Fines (%) (<0.075 mm)	92
Sand (%) (0.075-4.75 mm)	8
Atterberg limit (ASTM D4318)	
Liquid limit, LL (%)	29
Plastic limit, PL (%)	17
Plasticity index, PI (%)	12
USCS soil classification	CL
Compaction characteristics (ASTM D698)	
Maximum dry unit weight, γ_{dmax} (kN/m^3)	17.6
Optimum moisture content, ω_{opt} (%)	15.5

The bearing capacities of structures may decrease under the influence of natural hazards such as floods. When a flood occurs, water accumulates in the road's vicinity and cannot penetrate the underlying soil layers. This issue could lead to road immersion in the water for an extended period and diminish the strength and bearing capacity of the road.

In March 2020, a flood occurred in Khuzestan province, Iran. This phenomenon caused the roads and infrastructure to go under the water for different periods, between a week and three months. Fig. 1 shows a view of the Ahvaz-Shush road, one of the most important transportation roads in Khuzestan, Iran, submerged after the flood. The maximum. temperature during the day was 23° C and the minimum at night was 3°C. In this area, roads are constructed by embankments to avoid a run-off on the road (Khayat *et al.* 2021).

This research confirms the effectiveness of fly ash, GGBS, and lime in soil stabilization and highlights the critical role of curing conditions, particularly under varying temperature environments. Including ambient and cold temperature (3°C) curing in the study provides a novel perspective on how these materials behave in different climates, making the findings more relevant for infrastructure projects in regions subject to freezing temperatures. This aspect of the study, combined with the detailed microstructural analysis, adds significant value and originality to the soil stabilization field.

2. Materials

2.1 Soil

The soil used in this paper (Fig. 2(a)) was collected from Shush city in the Khuzestan province of Iran. According to the Unified Soil Classification System, it was classified as low plasticity clay, CL, with a liquid limit of 29% and a plasticity index of 12%. Fig. 3 presents the particle size gradation curves of soil and GGBS materials. Some geotechnical properties of clay soil are presented in Table 1.

The oxide composition of the materials used in this study is presented in Table 2.

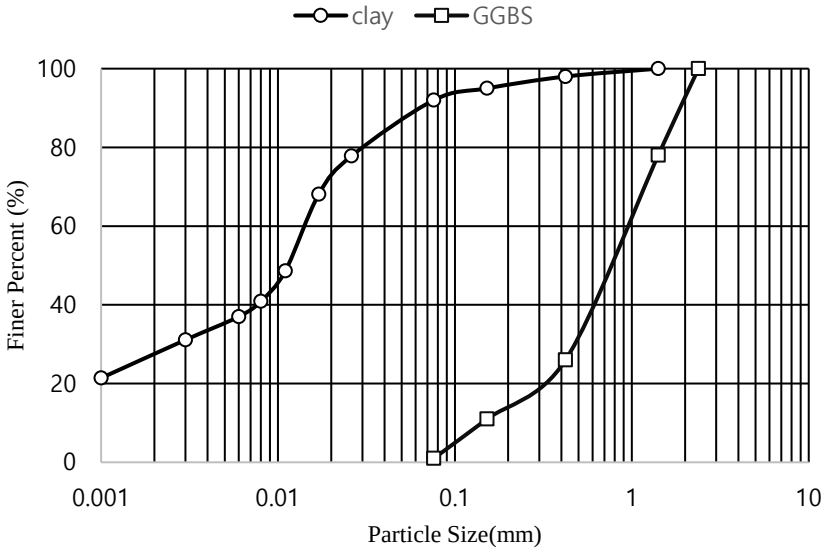

Fig. 3 Particle size distributions of soil

Table 3 Summary of UCS testing program

No.	Mix designation	GGBS (%)	Lime (%)	Fly ash (%)	Curing time (day)	Temperature conditions	Planned tests*
1	Untreated soil	0	0	0	1, 7, 14, 28, 56 and 90	ambient temperature (23 ± 2ºC) and 3°C	UCS tests at ambient temperature, UCS tests at 3°C, durability tests at ambient temperature, durability tests at 3°C
2	14%G*+2%F*	14	0	2			
3	12%G+2%L*+2%F	12	2	2			
4	10%G+4%L+2%F	10	4	2			
5	8%G+6%L+2%F	8	6	2			
6	6%G+8%L+2%F	6	8	2			
7	4%G+10%L+2%F	4	10	2			
8	2%G+12%L+2%F	2	12	2			
9	14%L+2%F	0	14	2			

* Each test was done with three repeats

* G: GGBS, F: Fly ash, L: Lime

2.2 GGBS

The GGBS was obtained from the Khuzestan Steel Company. It was pulverized and subjected to 40-grade sieves. Fig. 2(b) shows the GGBS. This study used GGBS mass contents of 0%, 2%, 4%, 6%, 8%, 10%, 12%, and 14% in the soil.

2.3 Lime

This study utilized powder quicklime with a density of 2.2 gr/cm^3, obtained from the Ahvaz factory in Ahvaz, Iran. Quicklime has higher water absorption than slaked lime. Therefore, it is more workable and can be easily stored. This study applied lime (Fig. 2(c)) mass contents of 0%, 2%, 4%, 6%, 8%, 10%, 12%, and 14% to the soil. The lime rates used in this study were selected based on scientific literature (Bao *et al*. 2022, Parhizkar *et al*. 2024, Alhakim *et al*. 2024; Fan *et al*. 2022,Amadi *et al.* 2021).

2.4 Fly ash

Fly ash is a non-crystalline amorphous powder form of silica with spherical particles (Ghorbani and Hasanzadehshooiili 2018) obtained from ferrosilicon production in electric arc furnaces. Since it is much more active than crystalline quartz, spherical silica participates more in pozzolanic reactions and shows more advantages than other pozzolans. This study obtained fly ash produced by Abadgaran Company, Ahvaz, Iran. Fly ash is a dark gray material (Fig. 2(d)) with 96% SiO_2 content. This study uses 2% of fly ash. This content was selected based on multiple studies investigating the optimal use of FA in soil stabilization (Parhizkar *et al.* 2024, Sharma and Hymavathi 2016).

3. Sample preparation

Table 3 summarizes the experimental program tests, and the code of each sample is also provided in this table. The

Table 4 Summary of Atterberg results and soil classification

No.	Mix designation	LL (%)	PL (%)	PI (%)	Soil Classification	MDU (kN/m^3)	OMC (%)
1	Untreated soil	29	17	12	CL	17.6	15.5
2	14%G+2%F	30	20	10	CL	17.9	15.0
3	12%G+2%L+2%F	37	28	9	ML	17.1	15.0
4	10%G+4%L+2%F	41	33	8	ML	17.0	17.5
5	8%G+6%L+2%F	46	39	7	ML	16.8	17.0
6	6%G+8%L+2%F	48	42	6	ML	16.5	18.0
7	4%G+10%L+2%F	50	44	6	MH	16.0	18.7
8	2%G+12%L+2%F	52	47	5	MH	15.6	21.0
9	14%L+2%F	54	50	4	MH	15.4	22.7

* G: GGBS, F: Fly ash, L: Lime

soil with materials (Lime + GGBS + Fly ash) was mixed, and the OMC and MDU were applied. An electrical blender was used to distribute water uniformly throughout the mixture. Then, the mixture was compacted using a static compactor. The cylindrical samples with a size of 5 cm diameter×10 cm height were extruded using a remolding jack. Then, they were placed within nylon bags to prevent heat transfer with the ambient and induce hydration in the samples. They were cured at ambient temperature (23 ± 2ºC) for 1, 7, 14, 28, 56, and 90 days before subjection to unconfined compressive strength (UCS) tests. The Unconfined Compressive Strength (UCS) tests were conducted in accordance with ASTM D2166.

To investigate the effect of temperature conditions on the stabilization process, another category of samples was refrigerated at 3°C for 1, 7, 14, 28, 56, and 90 days and subjected to UCS testing. Also, to investigate the effects of flood and strength in immersion conditions, three samples of each mix design were fabricated for durability tests at 28 days at ambient temperature (23 ± 2ºC) and 3°C. Then, the samples were immersed in water for four days and were subjected to compressive strength tests (Obuzor *et al*, 2012). Three replicates for each test were conducted. In the present study, a total of 378 tests, including 162 UCS tests on cured soil at ambient temperature (23 ± 2ºC), 162 UCS tests on cured soil at 3°C, 27 durability tests on cured soil at ambient temperature (23 ± 2ºC), and 27 durability tests on cured soil at 3° Carried out.

4. Results

4.1 Atterberg limits

Fig. 4(a) represents the Atterberg limits results for different contents of fly ash, lime, and GGBS. According to the results, the plastic and liquid limits grew as the lime content increased (Bell 1996). The soil with 14%L+2%F showed the highest increase in the liquid limit (1.86 times as large as that of the untreated soil). Adding 2% lime to untreated soil raised the liquid limit from 29 to 37. Furthermore, the liquid limit increased over time at higher lime contents. The soil with 14%G+2%F with no lime content showed a relatively small change in the liquid limit (83%) compared to untreated soil.

The highest plastic limit was found in the soil with 14%L+2%F, which experienced a 194% rise compared to the plastic limit of untreated soil. Similar to the liquid limit, adding 2% lime to untreated soil significantly raised the plastic limit (65%). The variations of the plastic limit became smaller at more significant lime contents. The sample with GGBS and fly ash without lime had an 18% higher plastic limit than untreated soil. Although it increased the limits for liquid and plastic, lime reduced the plasticity index (Zhu *et al*. 2019). The reduction of the plasticity index was also observable in the presence of GGBS.

Fig. 4(b) shows the Casagrande chart of the samples, and Table 4 provides the classification of the soils. The untreated soil and the sample with 14%G+2%F are classified into the group CL based on the USCS classification. According to Table 4, all the lime-containing samples have changed into silt. The soil is classified as ML at the lime contents of 2%, 4%, 6 %, and 8 %, while it is classified as MH at 10%, 12%, and 14%.

4.2 pH

Fig. 5 indicates the pH values of the samples. As can be seen, adding lime and GGBS to the untreated soil increased pH from 8.1 to 12.4. Expanding pH increases the formation of cementitious compounds and improves soil strength (Mwiti *et al*. 2018). An increase in pH provides the right conditions for dissolving the surface of soil particles. This is essential to release silica and alumina into the mixture and stimulate chemical reactions (Mohanty *et al*. 2021).

The addition of 2% lime expanded pH by 48%. A further rise in the lime weight content from 4% to 14% slightly increased pH (compared to the 2% sample) and led to a 53% higher pH than the untreated soil. Furthermore, GGBS and fly ash raised the pH of untreated soil by 30%. At pH values above 10.5, the structure of clay minerals breaks`, and a rise in the lime content increases pH to up to 12.4, following which silica and aluminum are released as C-S-H

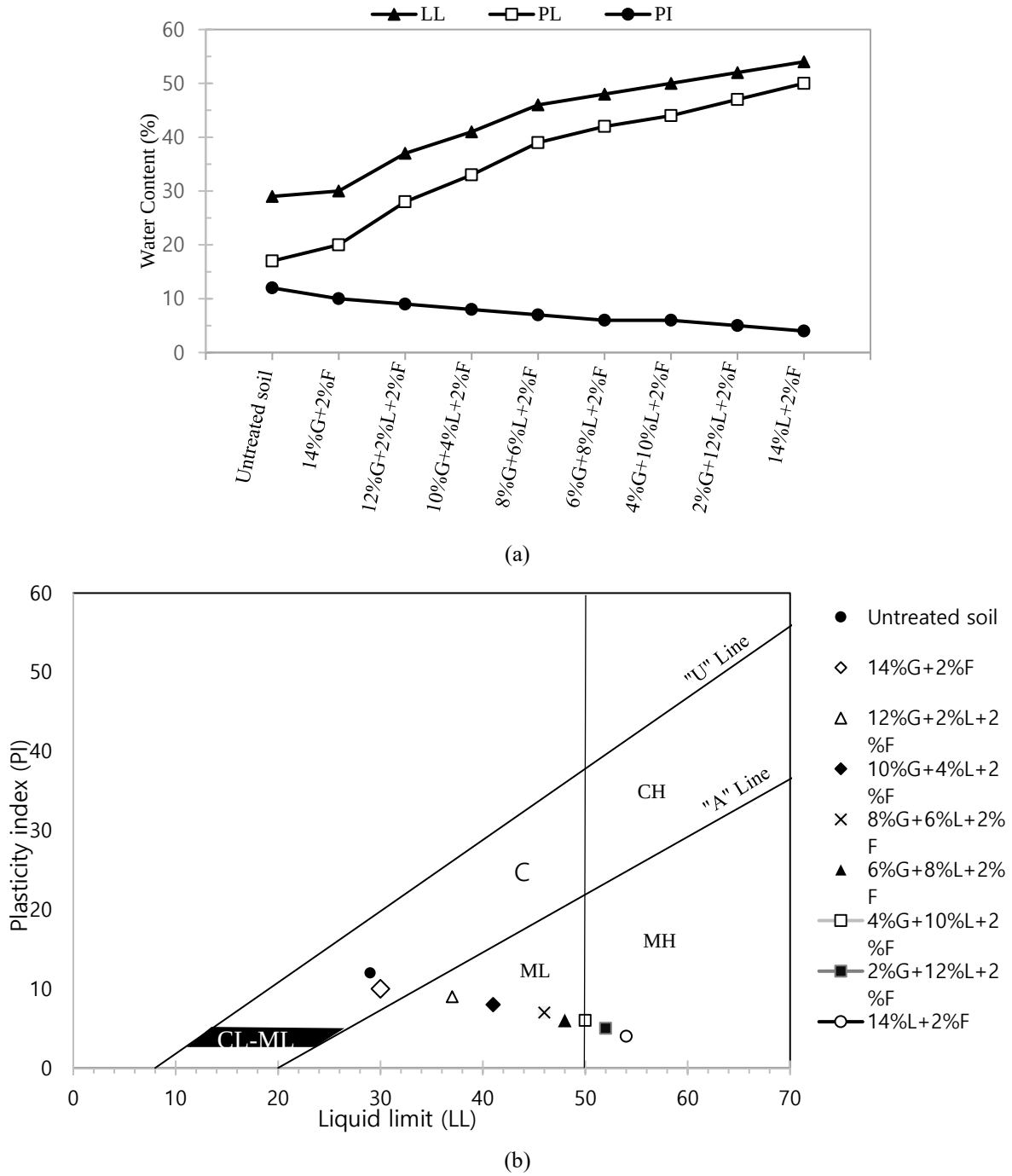

Fig. 4 (a) Atterberg values and (b) Casagrande's plasticity chart for the stabilized clay

and C-A-H gel products. These results reasonably agree with Islam *et al*. (2014).

4.3 Compaction tests

Fig. 6 provides the OMC and MDU values obtained from the standard proctor compaction tests at different GGBS, fly ash, and lime contents. According to Fig. 6, lime content increased MDU and reduced OMC compared to untreated soil. The sample with % lime content of 14% showed the most considerable MDU reduction (89% of the untreated soil's MDU). This issue can be attributed to the lower density of lime than soil. Furthermore, it can be said that the instant soil-lime reactions accumulate particles to occupy larger spaces. This result agreed with the previous study by Gao *et al*. (2016).

On the other hand, the sample with 2% fly ash + 14% GGBS directly affected the soil's MDU enhancement. As can be seen in Fig. 6, the sample with 14% GGBS showed a 1.02% higher MDU. These findings agree with previously published results by Mandal and Singh (2016).

OMC raised as the lime content increased. The most considerable OMC enhancement occurred in the sample with 14% lime (46% higher than the untreated soil). This

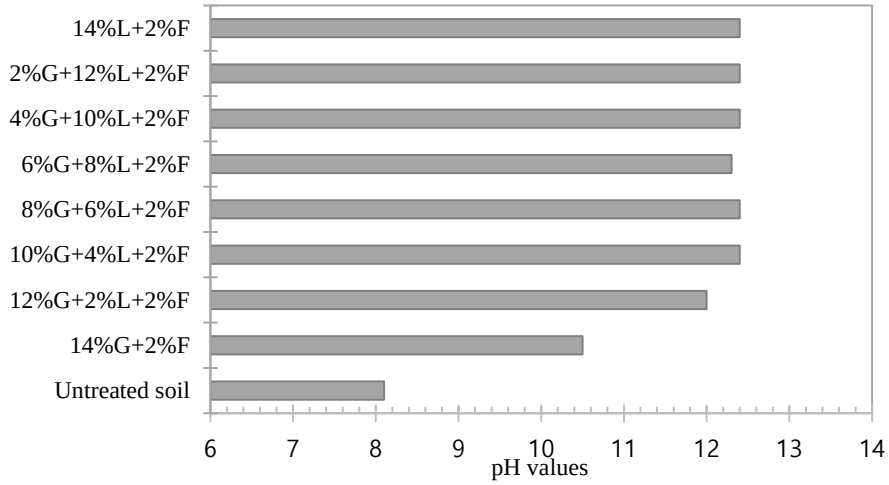

Fig. 5 Effect of lime, GGBS and fly ash content on pH of clay

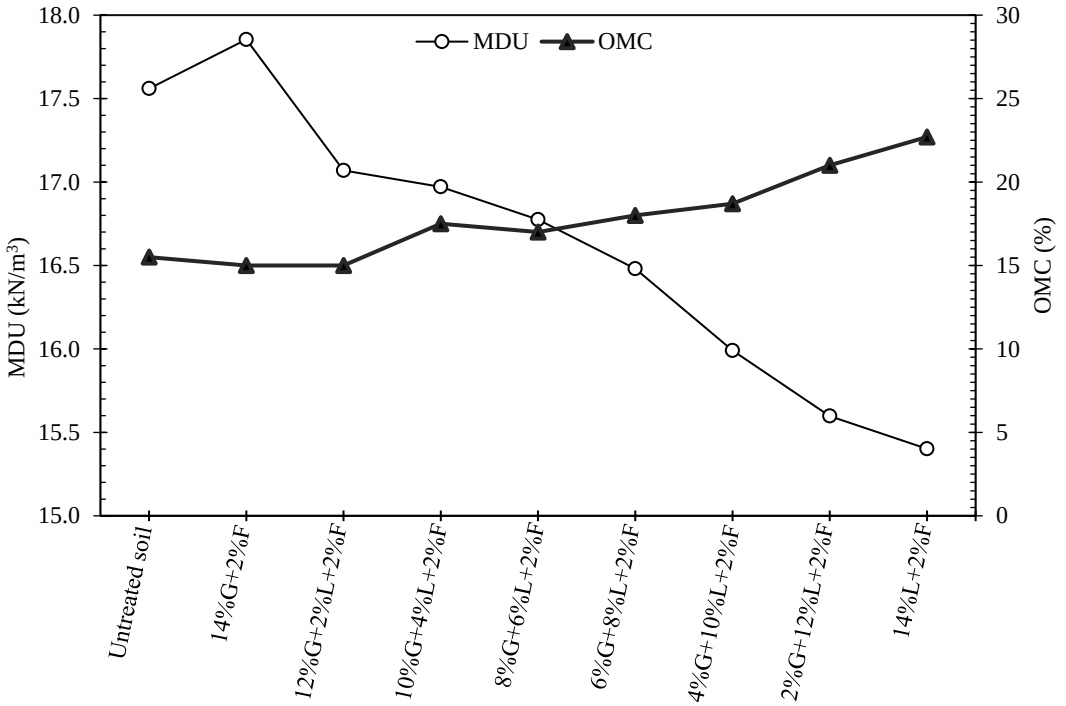

Fig. 6 Effect of lime, GGBS, and fly ash content on OMC and MDU of clay

issue can be attributed to the pozzolanic reaction between the soil and lime (Gao *et al.* 2016). On the other hand, according to Fig. 6, adding GGBS and fly ash decreased OMC by 0.97% of the untreated soil, possibly due to the replacement of clay fraction by non-plastic materials like fly ash and GGBS.

4.4 Unconfined compressive strength

Fig. 7(a) represents the UCS results of the stabilized soil samples with different contents of GGBS, lime, and 2% fly ash at the ambient temperature (23 ± 2º C) for 1, 7, 14, 28, 56, and 90 days. As can be seen, the UCS value increased with the curing age for most of the samples.

The sample contains 14% GGBS+2% fly ash compared to the untreated samples at curing times of 1, 7, 14, 28, 56, and 90 days, respectively, with 42, 44, 108, 40, 17, and 21% increases in UCS. The highest growth in UCS was at the curing age of 14 days when the sample UCS reached 2018 kPa. The UCS of the untreated soil at the same curing age was 969 kPa.

The soil sample with 8% GGBS+6% Lime+2% Fly ash showed the highest UCS compared to other samples with different additive percentages. The UCS results indicated a significant enhancement rate at the curing ages of up to 90 days. The soil sample with 8% G+6% L+2%F was observed to have the highest strength at all the curing ages compared with other stabilized samples. The samples with lime

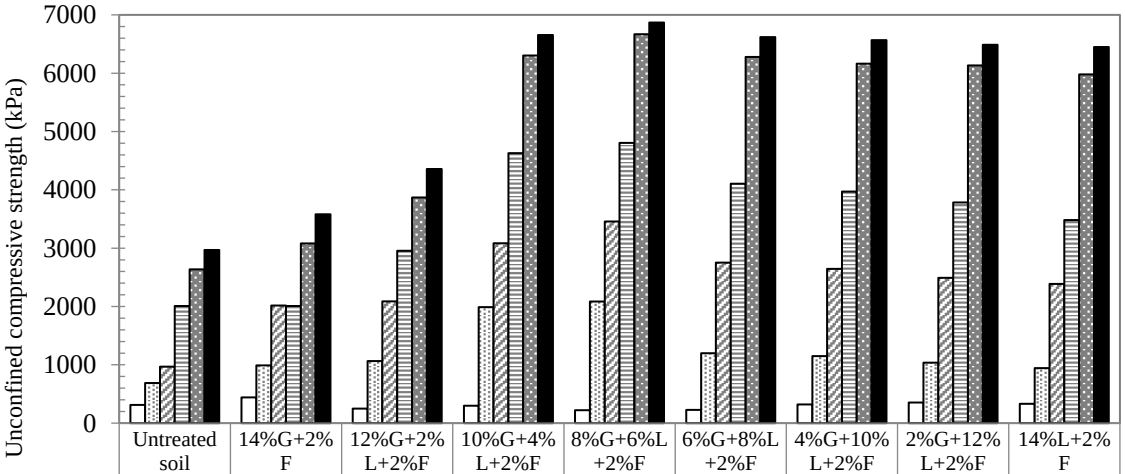

	Untreated soil	14%G+2% F	12%G+2% L+2%F	10%G+4% L+2%F	8%G+6%L +2%F	6%G+8%L +2%F	4%G+10% L+2%F	2%G+12% L+2%F	14%L+2% F
UCS(1-day curing)	312	443	248	297	222	228	322	353	333
UCS(7-days curing)	689	990	1066	1989	2086	1200	1151	1036	945
UCS(14-days curing)	969	2018	2089	3085	3458	2753	2645	2492	2386
UCS(28-days curing)	2009	2009	2955	4630	4806	4104	3972	3785	3481
UCS(56-days curing)	2637	3083	3868	6303	6668	6279	6163	6134	5979
UCS(90-days curing)	2970	3582	4359	6656	6869	6618	6567	6488	6449

(a)

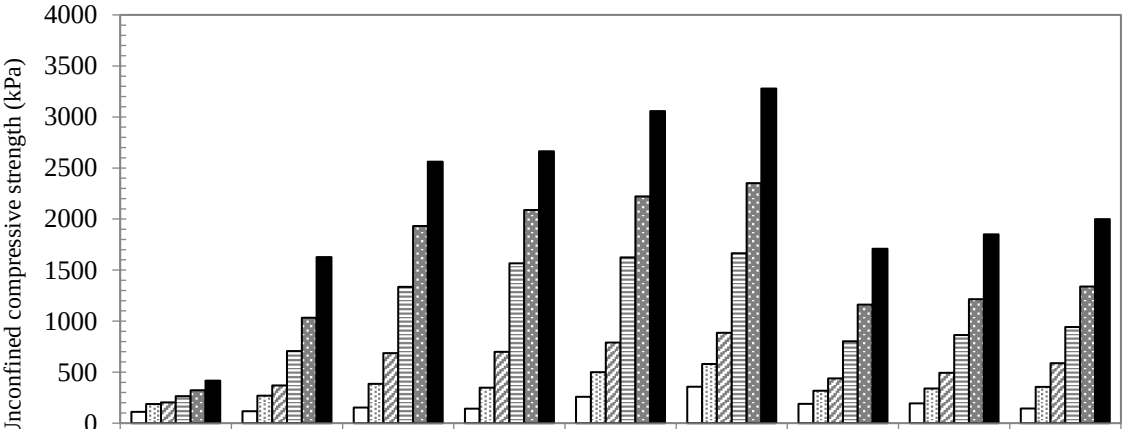

	Untreated soil	14%G+2% F	12%G+2% L+2%F	10%G+4% L+2%F	8%G+6%L +2%F	6%G+8%L +2%F	4%G+10% L+2%F	2%G+12% L+2%F	14%L+2% F
UCS(1-day curing)	111	118	153	142	258	357	189	194	144
UCS(7-days curing)	188	269	385	347	499	580	318	340	356
UCS(14-days curing)	204	369	686	700	790	885	438	494	588
UCS(28-days curing)	264	707	1336	1566	1624	1665	802	863	942
UCS(56-days curing)	323	1033	1932	2088	2222	2351	1161	1215	1339
UCS(90-days curing)	417	1628	2563	2663	3058	3279	1709	1851	1999

(b)

Fig. 7 Effect of lime, GGBS, and fly ash content on the strength of clay (a) at the ambient temperature and (b) at the 3ºC temperature

contents that were more significant than 6% experienced UCS reduction, and this reduction rate became even more extensive as the lime content increased. This result is in agreement with Chitragar *et al.* (2021). The UCS of soil mixed with adding 8% GGBS+6% Lime+2% Fly ash at 1-day curing is decreased by 29% compared to untreated soil.

This issue can be attributed to lime requiring time to engage in pozzolanic reactions, while 1 day of curing is insufficient. The UCS value of soil mixed with the addition of 8% GGBS+6% Lime+2% Fly ash compared to untreated soil is increased by 203, 257, 139, 153, and 131% after 7, 14, 28, 56, and 90 days of the curing period, respectively.

This emphasizes that a sufficient amount of lime is available for the dissolution of silica and alumina present in

(a) (b)

Fig. 8 View of durability test

the soil matrix and form cementitious compounds over the curing period (Sivapullaiah and Jha 2014). Strength enhancement is attributed to the development of cementitious products and pozzolanic reactions, which reduces pore volume because of cation exchange between calcium ions in lime or GGBS and clay minerals (Lekshmi and Sudhakumar 2022).

Fig. 7(b) represents the UCS results of the stabilized soil samples with different contents of GGBS, lime, and 2% fly ash at 3° C for 1, 7, 14, 28, 56, and 90 days. In all samples, UCS expanded with the increase in the curing age. It added 14% GGBS+2% Fly ash to the soil sample, with slightly risen UCS compared to the untreated soil. The sample contained 14% Lime + 2% Fly ash compared to the untreated samples and had an increment in UCS of 30, 89, 189, 257, 314, and 379% at curing times of 1, 7, 14, 28, 56, and 90 days, respectively.

The soil sample with 6% GGBS+8% Lime+2% Fly ash showed the highest UCS at the different curing periods. The UCS improved at a higher rate for the curing ages of up to 90 days, and it was also observed to have the highest strength at all the curing ages. The samples with lime contents that were more significant than 8% experienced UCS reduction, and this reduction rate became even more extensive as the lime content increased (Ismeik and Shaqour 2020). The UCS enhancement can also be ascribed to elevated cohesion (C), resulting from cementation and pozzolanic reactions between lime and fine-grained soil. These interactions create cementitious compounds that effectively unite soil particles. The UCS of soil mixed with the addition of 6% GGBS+8% Lime+2% Fly ash compared to untreated soil is increased by 222, 209, 335, 531, 627, and 686% after 1, 7, 14, 28, 56, and 90 days curing period, respectively.

4.5 Durability

According to Fig. 7, all the samples with lime content higher than 2% obtained more than 60% of UCS at 28 days. Therefore, according to (Obuzor *et al.* 2012), the durability tests were performed at the curing age of 28 days. It should be mentioned that the samples were placed in the water without coverage (Fig. 8).

The durability index (DI) is the UCS ratio of a sample with four days of post-curing immersion in water to that of the same sample at 28 days. It is calculated by Eq. (1).

$$DI(\%) = \frac{UCS_{saturation}}{UCS_{unsaturation}} \times 100 \quad (1)$$

Fig. 9(a) represents the durability test results at ambient temperature (23 ± 2ºC). As can be seen, the samples containing GGBS and lime had lower UCS reduction and higher performance than those containing either lime or GGBS. It can be said that lime induces pozzolanic reactions in the presence of GGBS and enhances soil strength. However, the pure clay sample without additives was destroyed due to water immersion. The sample with 6% GGBS+8% Lime+2% Fly ash showed the highest post-immersion UCS. Its UCS was approximately 19% lower than that of the unsaturated sample. It can be inferred that GGBS improves lime soil strength and durability. This finding agrees with (Asghari-Kaljahi et al, 2020).

Fig. 9(b) represents the durability test results at 3ºC. As can be seen, the samples containing GGBS and lime had lower UCS reduction and higher performance than those containing either GGBS. However, the untreated sample was destroyed due to water immersion. The soil sample with 6% GGBS +8% Lime +2% Fly ash showed the highest post-immersion UCS. Its UCS was approximately 11% lower than that of the unsaturated sample. It can be inferred that lime improves soil strength and durability in the presence of GGBS.

4.6 Mineralogical and micro-structural changes

The optimum sample with 8%G+6%L+2%F was selected after the UCS and durability tests. The samples were fabricated at different curing ages, and an untreated sample was used at 56 days to perform element analyses and identify the constituent phases using the FE-SEM test and energy-dispersive X-ray spectroscopy (EDS).

Fig. 10(a) illustrates the XRD peaks of the untreated

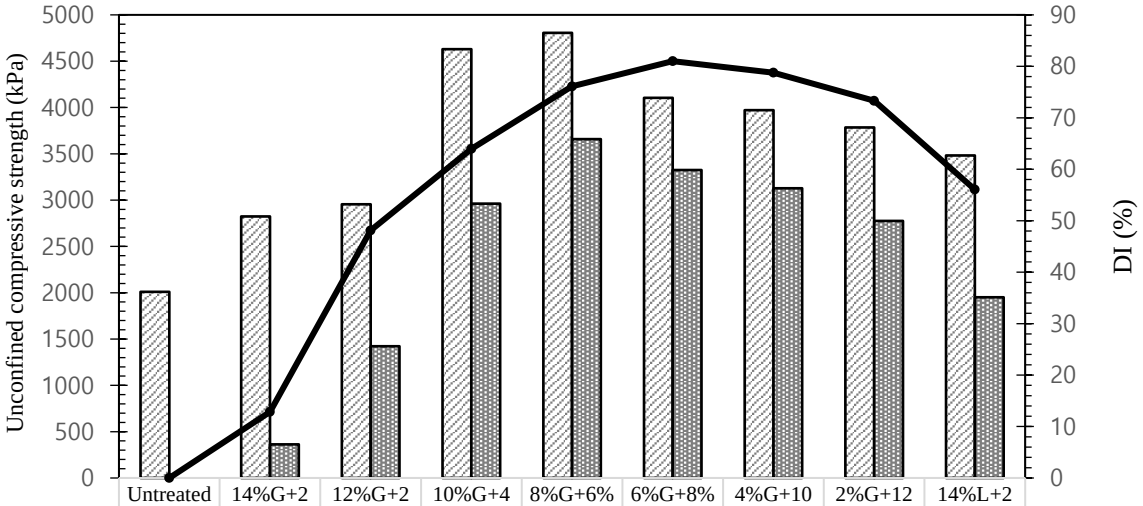

	Untreated soil	14%G+2%F	12%G+2%L+2%F	10%G+4%L+2%F	8%G+6%L+2%F	6%G+8%L+2%F	4%G+10%L+2%F	2%G+12%L+2%F	14%L+2%F
Unsaturated	2009	2823	2955	4630	4806	4104	3972	3785	3481
Saturated	0	363	1422	2962	3658	3324	3128	2775	1952
DI	0	13	48	64	76	81	79	73	56

(a)

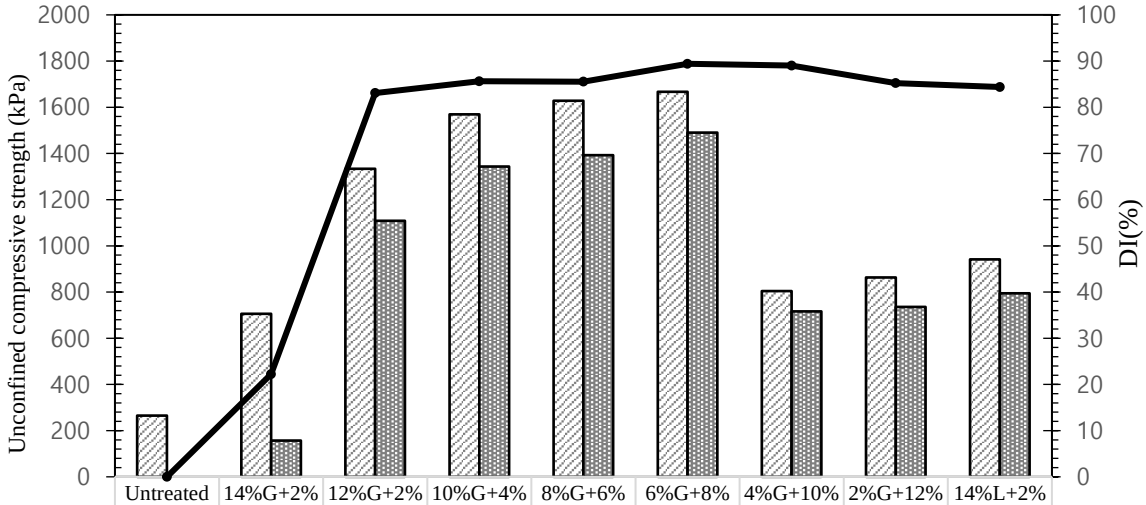

	Untreated soil	14%G+2%F	12%G+2%L+2%F	10%G+4%L+2%F	8%G+6%L+2%F	6%G+8%L+2%F	4%G+10%L+2%F	2%G+12%L+2%F	14%L+2%F
Unsaturated	265	706	1334	1569	1628	1667	804	863	941
Saturated	0	157	1108	1344	1393	1491	716	735	794
DI	0	22	83	86	86	89	89	85	84

(b)

Fig. 9 Effect of lime, GGBS and fly ash content on saturated and unsaturated clay (a) at the ambient temperature and (b) at the 3ºC temperature

sample, while Figs. 10(b)-10(d) shows the XRD graphs of the stabilized samples at the ages of 14, 28, and 56 days, respectively. Quartz, illite, and calcium carbonate exist in all the stabilized and untreated samples. The hydration products include C-A-S-H and C-S-H in Figs. 10(b)-10(d). Moreover, some reactions of clay minerals were weaker in the stabilized samples than in the untreated ones since the stabilized samples experienced pozzolanic reactions (Yi *et al.* 2015).

Fig. 7 shows that samples with lime contents below 8% showed higher strength. The largest UCS was found to occur in the sample with 8%G+6%L+2%F. This is attributed to the expanded C-S-H gel in the system due to increased silica and alumina (GGBS) in lime-induced alkaline conditions. Lime raises pH and activates GGBS, breaking the bonds of the Si-O and Al-O minerals and creating amorphous C-A-S-H gel and crystalline calcium aluminate hydrate. This enhances the strength of the soil (Dehghan *et al.* 2019).

Fig. 11 compares the FE-SEM images of the stabilized sample (soil sample with 8%G+6%L+2%F and soil sample with 6%G+8%L+2%F) and the untreated one Fig. 11(a)

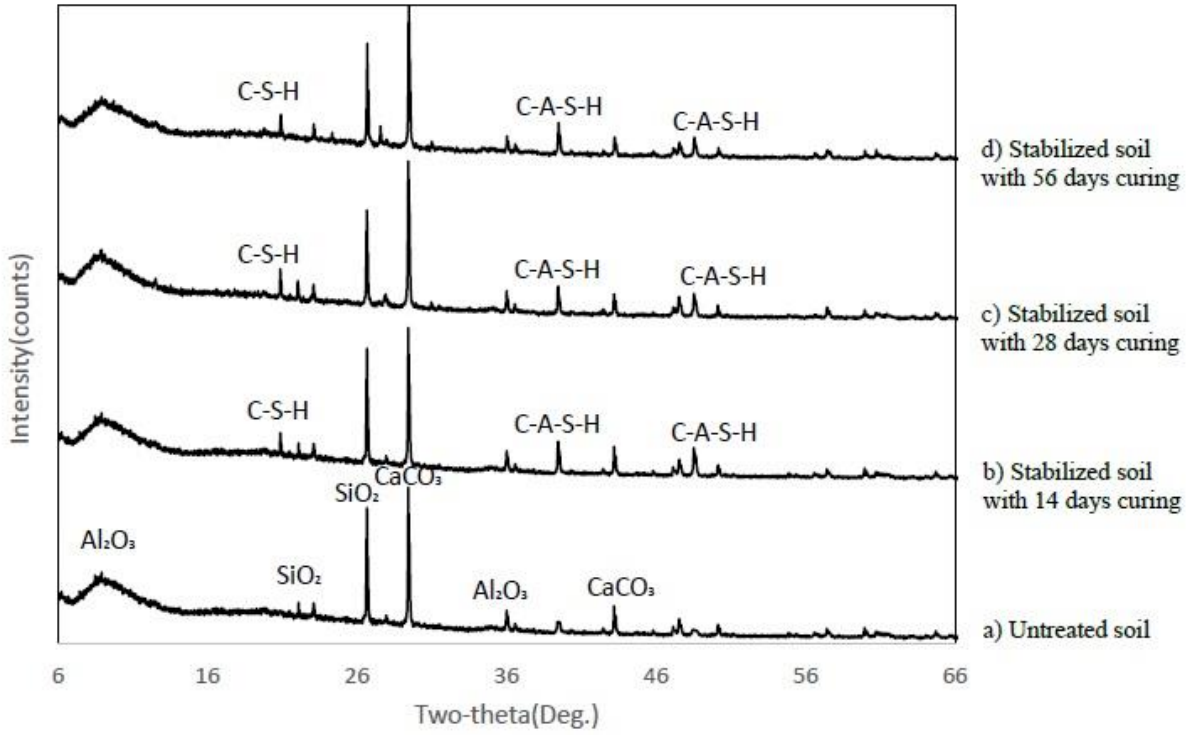

Fig. 10 XRD intensity counts for clay and stabilized clay at different curing times

shows the untreated sample with a porous, dispersed structure, and voids are observed. Figs. 11(b) and 11(c) shows the stabilized sample with 6%L+8%G+2%F after the age of 28 and 56 days at ambient temperature (23 ± 2ºC), and Figs. 11(d) and 11(e) shows the stabilized sample with 8%L+6%G+2%F after the age of 28 and 56 days at 3ºC.

Figs. 11(b) and 11(c) indicates the FE-SEM image of the stabilized sample at 28 and 56 days. Fewer and smaller voids are observed, suggesting a more compact structure. These images illustrate the hydration products formed in voids and flocculated structures, including C-A-S-H and C-S-H. Dehghan *et al*. (2019), Abdeldjouad *et al.* (2019) demonstrated that the linking C-A-S-H gel forms in voids contribute to forming more compact structures, improving compressive strength. This issue is in agreement with the XRD results.

In Figs. 11(d) and 11(e), the chemical remedy considerably modified the soil structure from porous to flocculated. Better cementing materials in the shape of crystalline products were located with longer curing ages, and the undulating shape of the untreated soil turned into now not as apparent. Using the XRF technique, those compounds were identified as calcium silicate hydrate (C-S-H) and calcium alumina silicate hydrate (C-A-S-H).

Energy-dispersive X-ray spectroscopy (EDS) analyses of particle surfaces are carried out on samples of the untreated sample and the stabilized samples with 6%L+8%G+2%F at the ages of 14, 28, and 56 days.

Fig. 12(a) shows the EDS of the untreated sample. Figs. 12(b) and 12(c)shows the EDS of the stabilized sample with 6%L+8%G+2%F after the age of 28 and 56 days at ambient temperature (23 ± 2ºC), and Figs. 12(d) and 12(e) shows the EDS of the stabilized sample with 8%lime+6%GGBS+2% fly ash after the age of 28 and 56 days at 3ºC.

The ionic ratios of the elements are presented in Table 5. The presence of silica, alumina, and calcium strongly supports the formation of cementitious compounds (C-S-H, C-A-S-H), confirming XRD analysis. The ratios of Al: Si, Al: Ca, and Ca: Si at the surface will carry out the modifications inside the composition of particle surfaces because of the coating of recent compounds shaped because of reactions that occur between the soil particles and additives (Sivapullaiah and Jha 2014). The CaO content of lime reacts with SiO2 and Al_2O_3 in clay to form cementation compounds. These mechanisms typically enhance UCS and reduce the plastic properties and swelling potential.

The chemical improvements are primarily driven by the pozzolanic reactions between the calcium hydroxide ($Ca(OH)_2$) from lime and the reactive silica (SiO_2) and alumina (Al_2O_3) present in the fly ash and GGBS. These reactions lead to cementitious compounds such as calcium silicate hydrate (C-S-H) and calcium aluminate silicate hydrate (C-A-S-H), significantly enhancing the soil's mechanical properties. The XRD spectra show the development of these compounds over the curing periods, with peaks corresponding to the presence of C-S-H and C-A-S-H, confirming the occurrence of these pozzolanic reactions.

As these hydration products form, they bind the soil particles together, reducing porosity and increasing the soil's overall compressive strength and durability. The transformation from free lime to stable cementitious

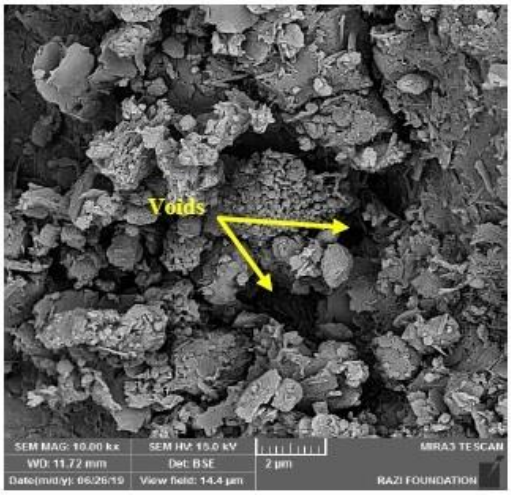

(a)

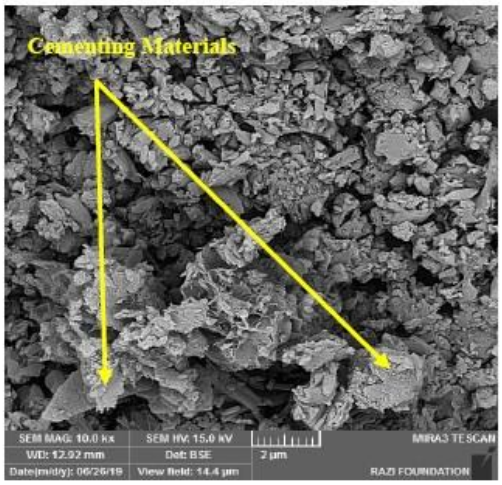

(b)

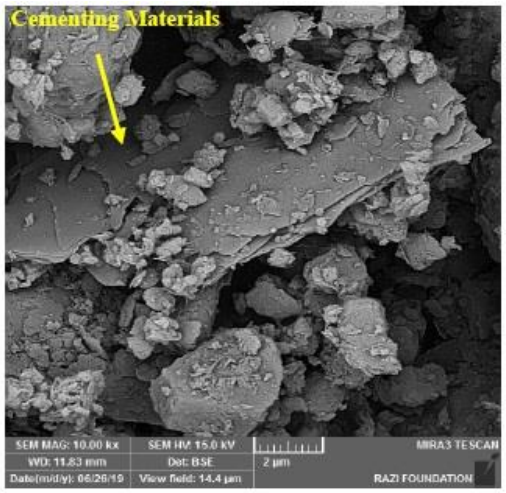

(c)

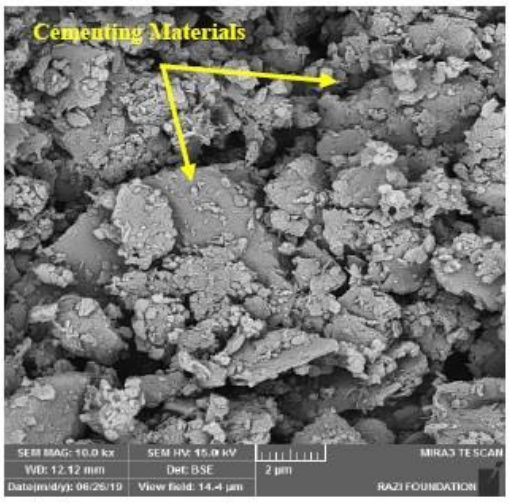

(d)

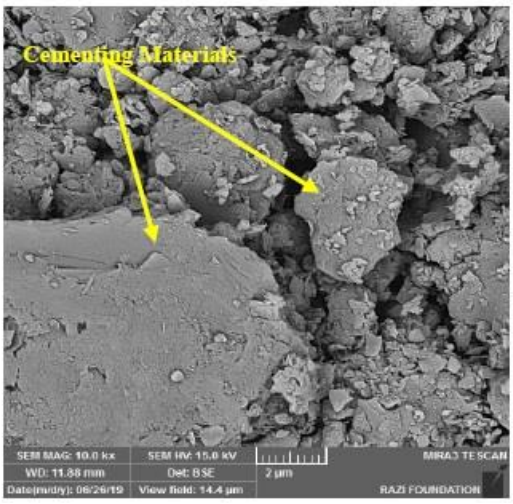

(e)

Fig. 11 FESEM image of (a) untreated clay, and stabilized clay at the ambient temperature cured for, (b) 28 days, and (c) 56 days and stabilized clay at the 3ºC temperature cured for: (d) 28 days, and (e) 56 days

materials also reduces the plasticity and swelling potential of the soil, further improving its geotechnical properties.

This is evident in the long-term strength gains observed in the unconfined compressive strength (UCS) tests, where stabilized samples exhibited significant increases compared to untreated soil. Similar observations have been made by Parhizkar *et al*. (2024) and Nasiri *et al*. (2021), where the formation of C-S-H and C-A-S-H contributed to substantial

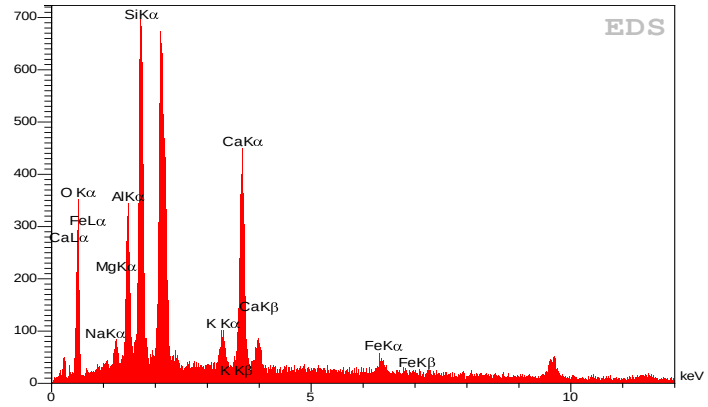

Fig. 12 EDS spectrums of (a) untreated clay and stabilized clay at the ambient temperature cured for (b) 28 days, and (c) 56 days and stabilized clay at the 3ºC temperature cured for (d) 28 days, and (e) 56 days

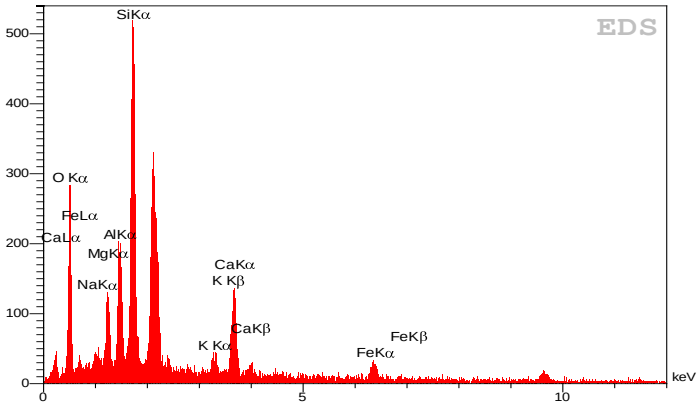

(e)

Fig. 12 Continued-

Table 5 EDAX analysis of soil and stabilized soil with 8% GGBS, 6 % lime, and 2% fly ash at 28 and 56 days curing times

Combinations	Curing time (day)	Al (atomic%)	Si (atomic%)	Ca (atomic%)	Al:Si	Al:Ca	Ca:Si
Untreated soil	56	3.78	10.5	1.9	0.36	1.99	0.18
8%G+6%L+2%F	28	5.62	13.73	12.94	0.41	0.43	0.94
	56	9.68	14.92	2.03	0.65	4.77	0.14

improvements in the mechanical properties of the stabilized soils.

The SEM analysis reveals significant physical improvements in the stabilized soil. The untreated soil displays a porous and loose structure with visible voids and weak particle bonding. However, the stabilized samples exhibit a much denser and more compact microstructure, with fewer and smaller voids. This densification is primarily due to the filling of pores by the hydration products (C-S-H and C-A-S-H) formed during the pozzolanic reactions.

The SEM images of the samples after 28 and 56 days of curing clearly show the reduction in pore spaces and the development of a more cohesive soil matrix. This densification increases the mechanical strength and improves the soil's resistance to water infiltration and erosion, making it more durable under flood conditions. The reduction in voids and the compact microstructure are consistent with findings from Sharma and Hymavathi (2016), who observed similar improvements in the soil structure when using fly ash and lime for stabilization.

Additionally, the interaction between fly ash particles and soil further enhances the soil's physical properties by promoting flocculation, which results in improved particle alignment and a stronger overall soil matrix. The reduction in void ratio and the enhanced particle cohesion are major factors contributing to the soil's long-term durability and stability, especially under varying environmental conditions.

The XRD data show that the untreated soil primarily consists of quartz and illite, with no significant cementitious phases. However, as the curing period progresses, the XRD spectra for the stabilized samples reveal the formation of new hydration products (C-S-H and C-A-S-H), indicating successful pozzolanic reactions. These compounds are crucial for improving soil strength and durability.

The SEM analysis supports these findings, visually demonstrating the physical changes in the soil's microstructure. The untreated soil's porous and weak structure contrasts sharply with the compact and solidified matrix observed in the stabilized samples. This transformation, facilitated by the chemical bonding between particles, results in a more durable and resistant soil with enhanced mechanical properties. The combination of chemical reactions and physical rearrangement of particles explains the significant improvements in soil performance.

5. Conclusions

The present study shows the characteristics of soils stabilized combinations of lime, GGBS, and fly ash to stabilize clay soil in two temperature conditions, ambient temperature (23 ± 2ºC) and 3ºC, and their effect on UCS, durability, and microstructural. Based on the experimental results obtained, the following conclusions can be drawn:

- The addition of 2% lime raised pH by 48%. A further rise in the lime weight content from 4% to 14% slightly raised pH (compared to the 2% sample) and led to a 53% higher pH than the untreated soil. Furthermore, GGBS and fly ash increase the pH of untreated soil by 30%.
- The Atterberg limits result showed that lime and GGBS changed soil classification from CL into ML and MH.

- According to compaction results, increasing the lime content raised MDU and reduced OMC compared to the untreated soil. The sample with % lime content of 14% showed the most MDU reduction (89% of the untreated soil MDU).
- Adding lime, GGBS, fly ash, and increased curing age changed the UCS of the samples.
- The durability test revealed that the untreated soil completely collapsed in water, while the stabilized samples showed sufficient strength after immersion in water.
- The sample with 8% GGBS+6% Lime+2% Fly ash at ambient temperature showed the highest UCS compared to others with different additive percentages. The UCS results indicated a high enhancement rate at the curing ages of up to 90 days. The UCS value improved at a lower rate for the curing ages above 56 days and showed the highest post-saturation strength.
- The sample with 6% GGBS+ 8% Lime+2% Fly ash at 3º C showed the highest UCS at the different curing periods. The UCS improved at a higher rate for the curing ages of up to 90 days. The sample with 6% GGBS+ 8% Lime+2% Fly ash showed it had the highest strength at all the curing ages and the greatest post-saturation strength.
- The microstructural tests demonstrated hydration products in the soil. The XRD results revealed the hydration products as the C-A-S-H and C-S-H gels. These products were also observed in the FE-SEM images, indicating good agreement between the tests.

Finally, this research aimed to develop a practical solution for road construction companies, professionals, and stakeholders to apply nontraditional additives to pavement sustainability, especially after the flood, and reduce related costs and decrease CO_2 emissions.

Acknowledgments

This investigation was carried out in the Advanced Soil Mechanics Laboratory, Islamic Azad University, Ahvaz, Iran.

References

Abdeldjouad, L., Asadi, A., B.K.Huat. B., Saleh Jaafar. M., Dheyab,.W. and Giuma Elkhebu, A. (2019), "Effect of curing temperature on the development of hard structure of alkali-activated soil", *Geomate J.*, **17**, 117-123. https://doi.org/10.21660/2019.60.8160.

Al Haffar, N., Fabbri, A. and McGregor, F. (2021), "Curing conditions impact on compressive strength development in cement stabilized compacted earth", *Mater. Struct.*, **54**, 103. https://doi.org/10.1617/s11527-021-01702-0.

Alavéz-Ramírez, R., Montes-García, P., Martínez-Reyes, J., Altamirano-Juárez, D.C. and Gochi-Ponce, Y. (2012), "The use of sugarcane bagasse ash and lime to improve the durability and mechanical properties of compacted soil blocks", *Constr. Build. Mater.*, **34**, 296-305. https://doi.org/10.1016/j.conbuildmat.2012.02.072.

Aldaood, A., Bouasker, M. and Al-Mukhtar, M. (2014), "Free swell potential of lime-treated gypseous soil", *Appl. Clay Sci*., **102**, 93-103. https://doi.org/10.1016/j.clay.2014.10.015.

Alhakim, G., Baalbaki, O. and Jaber, L. (2024), "Compaction and shear behaviors of sandy soil treated with lime and metakaolin", *Geotech. Geol. Eng.*, **42**(1), 79-95. https://doi.org/10.1007/s10706-023-02555-w.

Amadi, C.C., Okeke, O.C., Onyekuru, S.O., Okereke, C.N., Israel, H.O. and Ubechu, B.O. (2021), "Stabilization of expansive soils derived from Enugu shale in Enugu area, Southeastern Nigeria using lime, cement and coal fly ash admixtures", *Int. J. Innov. Sci. Res. Technol.*, **6**(11), 420-433.

Asghari-Kaljahi, E., Hosseinzadeh, Z. and Mansouri, H. (2020), "Treatment of clayey soils with steel furnace slag and lime for road construction in the South West of Iran", *In: Ameen, GeoMEast. Sustainable Civil Infrastructures*. Springer, Cham.., https://doi.org/10.1007/978-3-030-34199-2_5.

ASTM International. (2007), ASTM D422 Standard Test Method for Particle-Size Analysis of Soils.

ASTM International. (2010), ASTM D2166 - Standard test method for unconfined compressive strength of cohesive soil.

ASTM International. (2017), ASTM D4318 - Standard test methods for liquid limit, plastic limit, and plasticity index of soils. https://doi.org/10.1520/D4318-17.

ASTM International. (2021), ASTM D698 - Standard test methods for laboratory compaction characteristics of soil using standard effort (12, 400 ft-lbs./ft³ (600 kN-m/m³)). https://doi.org/10.1520/D0698-17.

Bao, W., Wang, H., Lai, H. and Chen, R. (2022), "Experimental study on strength characteristics and internal mineral changes of Lime-stabilized loess under High-Temperature", *Constr. Build. Mater.*, **351**, 128945. https://doi.org/10.1016/j.conbuildmat.2022.128945.

Behnood, A. (2018), "Soil and clay stabilization with calcium-and non-calcium-based additives: A state-of-the-art review of challenges, approaches and techniques", *Transport. Geotech*., **17**, 14-32. https://doi.org/10.1016/j.trgeo.2018.08.002.

Bell, F. (1996), "Lime stabilization of clay minerals and soils", *Eng. Geol*., **42**, 223-237. https://doi.org/10.1016/0013-7952(96)00028-2.

Bilgin, N., Yeprem, H.A., Arslan. S., Bilgin, A., Günay, E. and Marşoglu, M. (2012), "Use of waste marble powder in brick industry", *Constr. Build. Mater.*, **29**, 449-457. https://doi.org/10.1016/j.conbuildmat.2011.10.011

Bruno, A.W., Perlot, C., Mendes, J. and Gallipoli, D. (2018), "A microstructural insight into the hygro-mechanical behaviour of a stabilised hypercompacted earth", *Mater. Struct*., **51**(32), 1-17. https://doi.org/10.1617/s11527-018-1160-9.

Chen, L. and Lin, D.F. (2009), "Stabilization treatment of soft subgrade soil by sewage sludge ash and cement", *J. Hazard. Mater*., **162**, 321-327. https://doi.org/10.1016/j.jhazmat.2008.05.060.

Chenari, R.J., Fatahi, B., Ghorbani, A. and Alamoti, M.N. (2018), "Evaluation of strength properties of cement stabilized sand mixed with EPS beads and fly ash", *Geomech. Eng.*, **14**(6), 533-544. https://doi.org/10.12989/gae.2018.14.6.533.

Chitragar, S.F., Shivayogimath, C.B. and Mulangi, R.H. (2021), "Study on strength and volume change behavior of stabilized black cotton soil with different pH of soil-lime mixes for pavement subgrade", *Int. J. Pavement Res. Technol.*, **14**, 543-548. https://doi.org/10.1007/s42947-020-0117-x.

Cristelo, N., Glendinning, S., Fernandes, L. and Teixeira Pinto, A. (2013), "Effects of alkaline-activated fly ash and Portland cement on soft soil stabilisation", *Acta Geotech*., **8**, 395-405. https://doi.org/10.1007/s11440-012-0200-9.

Dehghan, H., Tabarsa, A., Latifi, N. and Bagheri, Y. (2019), "Use of xanthan and guar gums in soil strengthening", *Clean Technol. Environ. Policy*., **21**, 155-165. https://doi.org/10.1007/s10098-

018-1625-0.
Fan, W., Chen, W., Zhang, Q. and Wu, G. (2022), "Feasibility of protecting earthen sites with sticky rice and lime composite", *Constr. Build. Mater.*, **346**, 128449. https://doi.org/10.1016/j.conbuildmat.2022.128449.
Ferris, G., Eades, J., Graves, R. and McClellan, G. (1991), "Improved characteristics in sulfate soils treated with barium compounds before lime stabilization", *Transport. Res. Record*, **1295**, 45-51.
Gao, Y., Qian, H., Li, X., Chen, J. and Jia, H. (2016), "Effects of lime treatment on the hydraulic conductivity and microstructure of loess", *Environ. Earth Sci*., **77**, 1-15. https://doi.org/10.1007/s12665-018-7715-9.
Ghorbani, A. and Hasanzadehshooiili, H. (2018), "Prediction of UCS and CBR of microsilica-lime stabilized sulfate silty sand using ANN and EPR models; application to the deep soil mixing", *Soils Found*., **58**, 34-49. https://doi.org/10.1016/j.sandf.2017.11.002.
Gowthaman, S., Nawarathna, T.H.K., Nayanthara, P.G.N., Nakashima, K. and Kawasaki, S. (2021), "The amendments in typical microbial induced soil stabilization by low-grade chemicals, biopolymers and other additives: A review", *Build. Mater. Sustain. Ecol. Environ.*, 49-72. https://doi.org/10.1007/978-981-16-1706-5_4.
Haghighatjoo, S.M. and Zolfegharifar, S.Y. (2022), "Effects of fibre type and content on unconfined compressive strength of fibre-reinforced lime or cement-stabilised soils", *Geomech. Geoeng.*, **17**(6), 1962-1972. https://doi.org/10.1080/17486025.2021.1984589.
Islam, S., Haque, A. and Wilson, S. (2014), "Effects of curing environment on the strength and mineralogy of lime-GGBS–treated acid sulphate soils", *J. Mater. Civil Eng*., **26**, 1003-1008. https://doi.org/10.1061/(ASCE)MT.1943-5533.0000887.
Ismeik, M. and Shaqour, F. (2020), "Effectiveness of lime in stabilising subgrade soils subjected to freeze–thaw cycles", *Road Mater. Pavement Des.*, **21**(1), 42-60. https://doi.org/10.1080/14680629.2018.1479289.
Khayat, N. and Nasiri, H. (2023), "Study of strength characteristics and micro-structure analysis of soil stabilized with wastewater and polymer", *Int. J. Pavement Res. Technol.*, 1-12. https://doi.org/10.1007/s42947-023-00296-w.
Khayat, N., Nazarpour, A. and Ganjipour, S.S. (2021), "Application of lime Ground-Granulated Basic Furnace Slag (GGBS) in improving geotechnical properties of clayey soils in floodplain area, case study, Khuzestan Plain", *Adv. Appl. Geol*., **10**, 669-682. https://doi.org/10.22055/aag.2020.31309.2045.
Lang, L., Chen, B. and Li, N. (2021). "Utilization of lime/carbide slag-activated ground granulated blast-furnace slag for dredged sludge stabilization", *Mar. Georesour. Geotechnol.*, **39**, 659-669. https://doi.org/10.1080/1064119X.2020.1741050.
Lekshmi, S. and Sudhakumar, J. (2022), "An assessment on the durability performance of fly ash-clay based geopolymer mortar containing clay enhanced with lime and GGBS", *Cleaner Mater*., **5**, 100129. https://doi.org/10.1016/j.clema.2022.100129.
Mandal., S. and Singh, J. (2016), "Stabilization of soil using ground granulated blast furnace slag and fly ash", *IJIRSET*., **5**, 21121-21126. https://doi.org/10.15680/IJIRSET.2016.0512038.
Mishra, P., Shukla, S. and Mittal, A. (2022), "Stabilization of subgrade with expansive soil using agricultural and industrial by-products: A review". *Mater. Today: Proceedings*, **65**, 1418-1424.
Moayyeri, N., Oulapour, M. and Haghighi, A. (2019), "Study of geotechnical properties of a gypsiferous soil treated with lime and silica fume", *Geomech. Eng*., **17**(2), 195-206. https://doi.org/10.12989/gae.2019.17.2.195.
Mohanty, S.K., Pradhan, P.K. and Mohanty, C.R. (2017), "Stabilization of expansive soil using industrial wastes", *Geomech. Eng.*, **12**(1), 111-125. https://doi.org/10.12989/gae.2017.12.1.111.
Mohanty, S., Roy, N., Prasad Singh, S. and Sihag, P. (2021), "Strength and durability of flyash, GGBS and cement clinker stabilized dispersive soil", *Cold Reg. Sci. Technol.*, **191**, 103358. https://doi.org/10.1016/j.coldregions.2021.103358.
Mwiti, M.J., Thiong'o, J.K. and Muthengia, W.J. (2018), "Properties of activated blended cement containing high content of calcined clay", *Heliyon*, **4**(8), e00742. https://doi.org/10.1016/j.heliyon. 2018.e00742.
Nasiri, H., Khayat, N. and Mirzababaei, M. (2021), "Simple yet quick stabilization of clay using a waste byproduct", *Transport. Geotech.,* **28**, 100531. https://doi.org/10.1016/j.trgeo.2021.100531.
Obuzor, G., Kinuthia, J. and Robinson, R. (2012), "Soil stabilisation with lime-activated-GGBS—A mitigation to flooding effects on road structural layers/embankments constructed on floodplains", *Eng. Geol*., **151**, 112-119. https://doi.org/10.1016/j.enggeo.2012.09.010.
Pai, R.R., Patel, S. and Bakare, M.D. (2020), "Applicability of utilizing stabilized native soil as a subbase course in flexible pavement", *Ind. Geotech. J*., **50**, 289-299. https://doi.org/10.1007/s40098-020-00432-4.
Parhizkar, A., Nazarpour, A. and Khayat, N. (2024), "Investigation of geotechnical and microstructure characteristics of gypsum soil using ground granulated blast-furnace slag (GGBS), fly ash, and lime", *Constr. Build. Mater.*, **418**, 135358.
Ramesh, H.N., Kulkarni, M.G.R., Raghunandan, M.E. and Nethravathi, S. (2022), "Suitability of bagasse ash-lime mixture for the stabilization of black cotton soil", *Geomech. Eng.*, **28**(3), 255-263. https://doi.org/10.12989/gae.2022.28.3.255.
Rikmann, E., Zekker, I., Teppand, T., Pallav, V., Shanskiy, M., Mäeorg, U., Tenno, T., Burlakovs, J. and Liiv, J. (2021), "Relationship between phase composition and mechanical properties of peat soils stabilized using oil shale ash and pozzolanic additive", *Water*, **13**(7), 942. https://doi.org/10.3390/w13070942.
Sharma, R.K. and Hymavathi, J. (2016), "Effect of fly ash, construction demolition waste and lime on geotechnical characteristics of a clayey soil: A comparative study", *Environ. Earth Sci.*, **75**, 1-11.
Sivapullaiah, P. and Jha, A.K. (2014), "Gypsum induced strength behaviour of fly ash-lime stabilized expansive soil", *Geotech. Geol. Eng*., **32**, 1261-1273. https://doi.org/10.1007/s10706-014-9799-7
Sukprasert, S., Hoy, M., Horpibulsuk, S., Arulrajah, A., Rashid, A.S.A. and Nazir, R. (2021), "Fly ash based geopolymer stabilisation of silty clay/blast furnace slag for subgrade applications", *Road Mater. Pavement Des*., **22**, 357-371. https://doi.org/10.1080/14680629.2019.1621190.
Syed, M. and GuhaRay, A. (2020), "Effect of fiber reinforcement on mechanical behavior of alkali-activated binder-treated expansive soil: Reliability-based approach", *Int. J. Geomech.*, **20**(12). https://doi.org/10.1061/(ASCE)GM.1943-5622.0001871.
Thomas, A., Tripathi, R.K. and Yadu, L.K. (2019), "Alkali-activated GGBS and enzyme on the swelling properties of sulfate bearing soil", *Geomech. Eng.*, **19**(1), 21-28. https://doi.org/10.12989/gae.2019.19.1.021.
Yi, Y., Gu, L. and Liu, S. (2015), "Microstructural and mechanical properties of marine soft clay stabilized by lime-activated ground granulated blastfurnace slag", *Appl. Clay Sci.*, **103**, 71-76. https://doi.org/10.1016/j.clay.2014.11.005.
Zhu, F., Li, Z., Dong, W. and Ou, Y. (2019), "Geotechnical properties and microstructure of lime-stabilized silt clay", *Bull. Eng. Geol. Environ*., **78**, 2345-2354.

https://doi.org/10.1007/s10064-018-1307-5.
Zhuang, S. and Wang, Q. (2021), "Inhibition mechanisms of steel slag on the early-age hydration of cement", *Cement Concrete Res.*, **140**, 106283. https://doi.org/10.1016/j.cemconres.2020.106283.

GC